Preprint 19th European Photovoltaic Solar Energy Conference, 7-11 June 2004, Paris, France

BURIED CONTACT SOLAR CELL PROCESS MONITORING USING LOCK-IN THERMOGRAPHY

Jayaprasad Arumughan, Thomas Pernau
University of Konstanz, Department of Physics, P.O.Box X916, D-78457 Konstanz, Germany
Tel: +49-7531-88-4374, Fax: +49-7531-88-3895 E-mail: thomas.pernau@uni-konstanz.de

ABSTRACT: In this contribution we present latest results on buried contact solar cell process monitoring using light-modulated lock-in thermography.
Conventional lock-in thermography of solar cells is performed by applying a modulated bias voltage to the sample and a signal processing of the recorded thermal images following a lock-in technique. The result is a thermal image, where heat represents current flow across resistor, e.g. shunts. However this requires electrical contacting of the samples which is not applicable to the early processing stages of a solar cell.
The problem is overcome by providing the modulation required for the lock-in technique by modulated light, which is converted to the necessary modulated current by the sample. The light modulated lock-in thermography (LimoLIT) does not require any electrical contacts to the samples to be investigated. The only prerequisite for LimoLIT is a sample with a p/n junction, which is typically one of the early stages in solar cell manufacturing.
Buried contact solar cells sized 12.5*12.5 cm² were produced according to a typical buried contact solar cell process sequence. Each critical processing step was monitored by LimoLIT measurements on selected samples. The readily processed solar cells were passed through extended IV, thermography and light beam induced current measurement analysis. LimoLIT measurements after early process stages already detected the shunts which were most relevant for the completely processed solar cells. Deteriorating shunts could be tracked and in any LimoLIT measurement during the solar cell process. The extended analysis of the readily processed solar cells revealed that the dominating shunts were of diode-like nature, correlating with areas of high dislocation density in the silicon wafer material. This diode like behaviour complicated the fitting of the dark and illuminated IV curves. The shunt resistance values calculated from the dark IV curve did not correlate with the solar cell behaviour. Minor Ohmic shunts were found on the backside of the solar cells, where screen-printed aluminium produces line-shaped shunts at the aluminium/emitter interface. These Ohmic shunts can be reduced if silicon nitride acts as isolation layer, but the coated area has to be well-defined.
Keywords:- Buried Contact Solar Cell – 1, Lock-in Thermography – 2, Shunts - 3

1 INTRODUCTION

The development of multicrystalline silicon buried contact solar cells (BCSC) are of great interest due to the coast reduction of cell modules. The main concern regarding the BCSC process is the number of high temperature steps involved in it. The high temperature process not only increases the thermal budget of the BCSC but also the high probability of shunt incorporation during the process. Some aspects of shunt incorporation during BCSC process using lock-in thermography analysis to reveal the origin of shunts are done in this work. In addition, conventional voltage biased lock-in thermography measurement is carried out to study the nature of shunts. In this experiment, a buried contact solar cell process as described in [1] was employed, with minor modifications.

2 BCSC PROCESS

The process sequence is shown in figure 1. The shunt incorporation in buried contact solar cell was monitored using the light-modulated lock-in thermography (LimoLIT) technique at each relevant processing stage of the BCSC. The measurements were carried out on selected wafers after each high temperature step where the probability of shunt incorporation in BCSC is very high.
Plasma etching for edge isolation was carried out after the shallow emitter formation. As the plasma treated edges are covered with LPCVD silicon nitride (SiN_x) in the next step, a good surface passivation of the edges can be achieved which reduces I_{02}. The SiN_x layer will also prevent doping of the edges by the strong emitter diffusion.

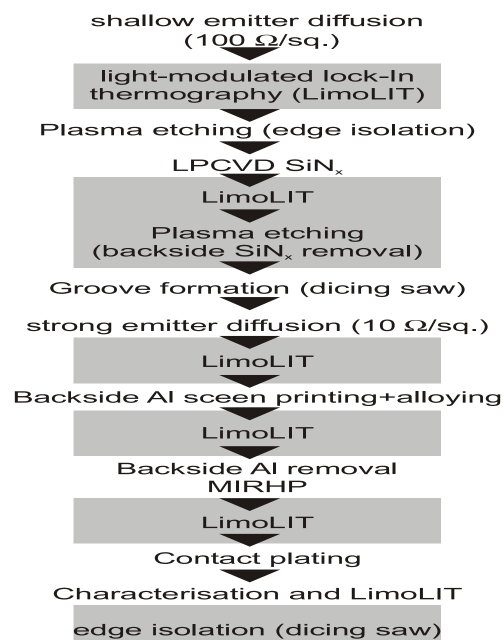

Figure 1: Process sequence used for BCSC fabrication and hence to study the shunt incorporation effects. A lock-in thermography analysis is carried out after each high temperature step to detect the shunt incorporation.

Due to the nature of the LPCVD SiN_x deposition process there is always some SiN_x coating on the rear side of the

wafers placed back-to-back for single-sided deposition. To investigate the contribution of this ''unwanted'' SiN_x deposition, one more plasma etching step is used on selected wafers to remove the residue coating. This affects also the edges, the coating thickness is reduced from 130 nm to 60 nm or below (nearly invisible to the naked eye). In the next step the contact grooves are created using a dicing saw equipped with a blade of thickness 15 µm. For further details see reference [1]. The back surface field (BSF) is formed by screen printing and firing of a conventional Al paste. The selection of the paste is made in such a way that the frits contained therein improve the depth of the BSF. To apply the Microwave Induced Remote Hydrogen Passivation (MIRHP) and electroless plating effectively, the aluminium rear contact is removed before passivation. This does not affect the heavily doped p^{++} region on the rear side, as only metallic aluminium and no Al-Si eutectic can be etched selectively with HCl [1].

3 LIGHT MODULATED LOCK-IN THERMOGRAPHY (LIMOLIT) METHOD

The light-modulated lock-in thermography is an enhancement of the conventional lock-in thermography (LIT). In conventional lock-in thermography, a modulated bias voltage is applied to the solar cell, and the thermal image of the solar cell is computed using a Lock-In technique [2]. This requires an electrical contact to the sample and is therefore restricted to completely processed solar cells. The LimoLIT method uses the capability of a photosensitive device to convert incident light into an electric current. By applying modulated light, the modulated bias voltage necessary for lock-in thermography is generated internally by the sample itself. This is also applicable to early processing stages of a solar cell, as soon as the device has a carrier separating p/n junction. More details about this method will be submitted in a dedicated contribution to this conference [3].

4 THE LIMOLIT ANALYSIS

In figure 2, the presence of shunts after the shallow emitter formation can be detected from the LimoLIT maps.
These shunts arise due to the strongly recombinative crystal defects in the multicrystalline silicon material. The LimoLIT method can detect these shunts after the formation of a p/n junction. A similar phenomenon was observed on other samples after the heavy phosphorous diffusion (See the µ-PCD lifetime map in figure 6 to identify the defected areas). Unfortunately we don't have a thermogram of the sample in figure 2 after heavy diffusion. Structures found already in early process stages can be identified throughout the process until the final process step (see ellipses).
The presence of linear shunts at the edges is detected after the third high temperature step, screen printing on the rear side and alloying. However the linear shunts were absent in the cells that have a protective SiN_x at the edges after plasma edge isolation. The signal strength of the latter is rather weak compared to the other shunt structures. Having a look at the signal phase delay, it is obvious that these shunts are located on the backside of the cell. Therefore it is possible that the front side thermogram underestimates the impact of these linear shunts.
The presence of linear edge shunts can be contributed to the presence of aluminium at the tip of an inter-digitated p/n junction on the rear side: after firing, a non uniform interface between BSF (p^{++} doped region) and the emitter is formed near the edges on the rear side. This produces an enlarged interface area with increased possibility for direct contacting between Al clusters and emitter [4, section 3.4]. Though this happens on a microscopic scale, it will produce locally confined shunts. A solar cell model describing various shunt types in BCSC is given in reference [5].

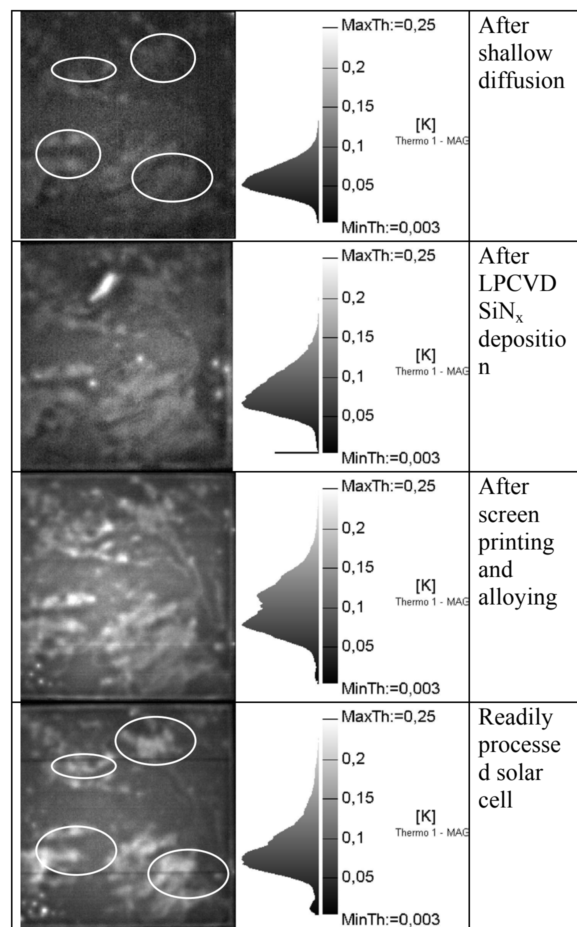

Figure 2: Shunt tracking by a sequence of LimoLIT measurements after high temperature steps in the processing sequence. The structures marked with the yellow ellipses in the first image can be identified throughout the whole process. These apparently material induced shunts contribute to R_p = 210 Ωcm² of this solar cell made from PV Silicon multicrystalline material.

The BCSC in figure 2 is a representative for those samples with "unwanted'' SiN_x on the back side which was not removed. For these solar cells, the rear n-p^{++} junction is partly isolated by the smooth border of the SiN_x covered area. This reduces the probability of shunting on the back side. Alternatively, the short-circuited margin can be removed by ample edge isolation

using the dicing saw. However the edge isolation step using the saw is not an absolute solution to remove the edge shunts. New shunts may be introduced due to the saw damage formed by cutting off the edges.

5 ILLUMINATED AND DARK IV MEASUREMENT

IV measurements of all the cells were carried out before the edge isolation using the dicing saw. The cell with highest efficiency (16 %) is the sample fabricated using Baysix multicrystalline material without removing SiN_x at the edges. The PV silicon multicrystalline material has also shown a comparable efficiency value of 15.1%. The evaluation of the shunt resistance R_p from the dark IV curves gave incredibly high values, see results in table 1.

Table I: Average shunt resistance values R_p for each 5 neighbouring Baysix wafers. The values calculated from the dark IV curve are incredibly high.

	Edge SiN_x removed	Edge SiN_x not removed
R_p dark [Ωcm²]	9037	11227
R_p illuminated [Ωcm²]	402	1213

The extreme differences of the shunt resistance between dark and illuminated measurements can only arise from diode or Schottky type behaviour of the shunts. The shunting diodes are only detectable in the illuminated case, i.e. when the solar cell is internally biased by its own photocurrent.

Table II: The edge isolated cell still suffers from the shunts near the edges. The removal of these parasitic shunts brings further improvement in cell parameters.

Area cm²	FF%	J_{sc} mA/cm²	V_{oc} mV	Eta %	R_p Ωcm²
156.25	77.4	32.9	626.6	16	2850
144	78.4	33.6	627.8	16.6	6723

In order to analyse the parasitic effect of the shunts near the edges (detected using LIT measurements) an additional, second, edge isolation is carried out. The volume shunts removed during the second edge isolation step helped to improve the cell parameters. These results are shown in table 2. The improvement in solar cell parameters is clearly due to the removal of the shunts *near* the edges (not *at* the edges).

6 LOCK-IN THERMOGRAPHY ANALYSIS

To investigate the Schottky behaviour in detail, conventional lock-in thermography measurements of the sample from figure 2 were performed using three different bias voltages of –0.5 V, 0 V and +0.5 V and a modulation of ±0.25 V. The results are shown in figure 3.The conventional lock-in thermograms are useful to clearly identify the nature of the shunts by applying a constant voltage bias. As long as the voltage bias is below 0.6 V in forward direction, the solar cell can produce heat only in the shunted regions. Ohmic shunts behave linearly and show the same power dissipation regardless of the bias voltage polarity. Diode-like shunts will only show up under forward bias, so it is even possible to determine their polarity.

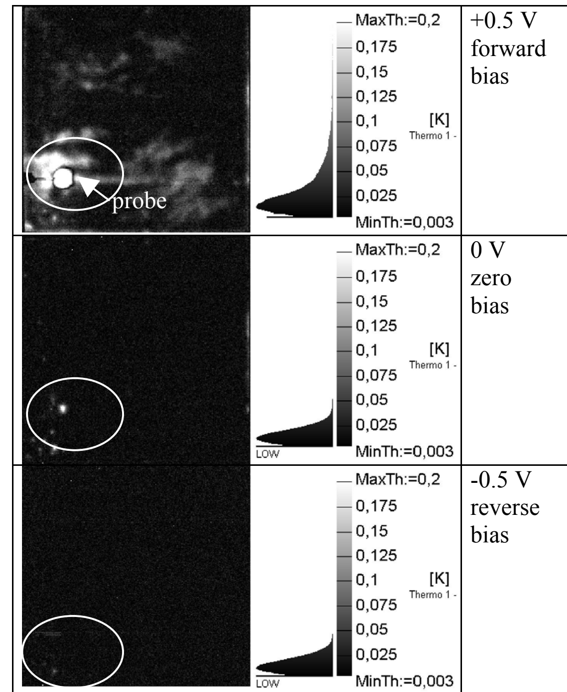

Figure 3: Conventional lock-in thermography measurements of the cell already shown in figure 2. The Ohmic shunts are visible in the zero biased measurement exclusively, whereas the forward biased measurement shows both diode-like and Ohmic shunts. The reverse biased measurement is to clearly identify the areas with diode-like behaviour. The ellipse is for comparison with the LBIC map in figure 5

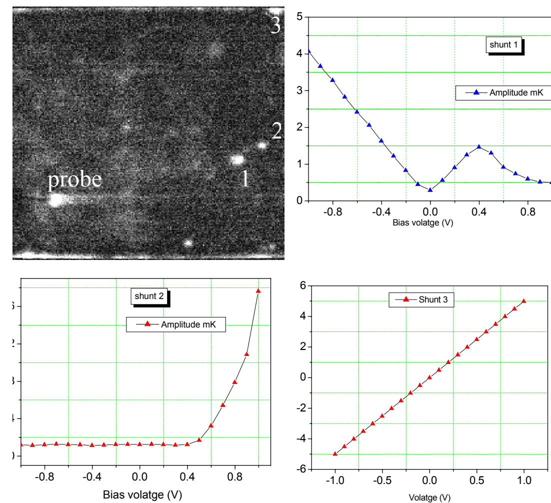

Figure 4: Shunt characterisation using voltage biased thermography measurements. The volume shunts 1 and 2 are Ohmic and Schottky types respectively. The linear shunt (numbered 3) is Ohmic in nature.

The nature of shunt can be analysed by plotting the amplitude values for reverse and forward biased conditions. Such a graph is given in figure 4. The top

right diagram is the amplitude versus voltage curve of a volume shunt numbered 1.The shape of the curve is explained in the following way. During the reverse bias, the p-n junction of the solar cell offers very high resistance. Hence all the current flows through the shunt resistance. There is a dip in amplitude values during the forward bias. This could be due to the low resistance offered by the junction after overcoming the knee voltage. The low forward resistance offered by the junction reduces the effective resistance of the shunt and junction system. This results in the appearance of the whole voltage across the series resistance of the cell. Hence the Ohmic shunts exhibits low signals in these forward bias voltage ranges. The volume shunt numbered 2 shows Schottky nature while the linear edge shunt 3 is Ohmic in nature.

7 LIGHT BEAM INDUCED CURRENT AND LIFE TIME ANALYSIS

Light beam induced current maps (LBIC) of the readily processed solar cells were recorded to collect information about the local current generation. There is a clear correlation between areas with high dislocation density (weak LBIC signal) and diode like shunts (strong thermal signal), see e.g. the areas marked with an ellipse in figures 3&4. The linear shunts at the edges are not visible in the LBIC map, i.e. they are weaker than the diode-like shunts. Also the point-shaped Ohmic shunts on bottom left of the thermograms cannot be identified in the LBIC map. The long-wavelength LBIC-map overestimated the current losses due to the missing BSF in the backside SiN_x covered regions.

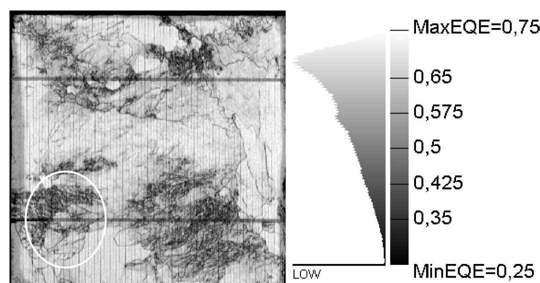

Figure 5: LBIC map (λ=980 nm, P_{opt}=1.5 μW) of the solar cell known from figures 2&3. The area marked with an ellipse can also be identified in figure 3. The marginal green areas are the regions covered with SiN_x on the back side. The coating inhibits the formation of the p^{++}-doped BSF.

Microwave photo conductive decay (μ-PCD) measurement was carried out to identify the areas with low carrier lifetime on the multicrystalline silicon material. A μ-PCD measurement carried out on a PV Silicon wafer is given in figure 6. The defected areas in the material can be identified using the scale provided in the same figure.

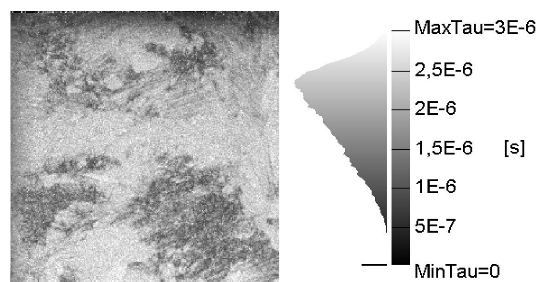

Figure 6: Lifetime map of a multi crystalline silicon (as cut) wafer. PV Silicon.

The regions with low life time have low EQE values as noted from the LBIC map. In addition it is clear that strongly recombinative crystal defects can invoke the formation of shunts.

8 CONCLUSIONS

We carried out a study to analyse the shunt incorporation in mc-Si buried contact solar cells by employing two different process sequences and three materials. Lock-in thermography analysis shows that the cells fabricated without removing the backside SiN_x have weaker linear shunts at the edges as compared to the cells which had the SiN_x removed. The "unwanted'' SiN_x has found have some beneficial effect. It preserves the edge isolation and prevents the formation linear edge shunts. In addititon the highest parallel resistance was obtained for the cell covered with silicon nitride after edge isolation. The shunt tracking using the LimoLIT technique showed that many of the defects found in early process stages of the solar cells can be identified in the completely processed solar cell later on. The majority of the shunts found showed diode-like and (or) Ohmic behaviour. Most of the shunts are located in areas with high dislocation density.

9 ACKNOWLEDGEMENTS

Authors would like to thank Mrs. Nidia Gawehns for providing technical assistance and Mr. Joris Libal and Mr. Alwin Trummer for μ-PCD measurements.

10 REFERENCES

[1] W. Joos, B. Fischer, P. Fath, S. Roberts, T. M. Bruton, Conference on PV in Europe from PV technology to Energy Solutions 2002 Rome
[2] O. Breitenstein, M. Langenkamp, J. P. Rakotoniaina, J. Zettner, Proc. 17 th EPSEC München (2001), p1499-1502
[3] M. Käs, S. Seren, T. Pernau, G. Hahn, 'LimoLIT – A novel Thermographic Characterisation Method for p/n Structures and Solar Cells', this conference.
[4] K. Faika, PhD thesis, electronic version at: http :// www.ub.unikonstanz.de/kops/volltexte/2003/1064/
[5] A. Jayaprasad, T. Pernau, A. Hauser, I. Melnyk 'Simplified edge isolation of buried contact solar cells' Proc. SCELL 2004, Badajoz.